

Chemoselective Hydrogenation of Crotonaldehyde Catalyzed by an Au@ZIF-8 Composite

Casey J. Stephenson,^[a] Cassandra L. Whitford,^[b] Peter C. Stair,^[a] Omar K. Farha,^{*,[a, c]} and Joseph T. Hupp^{*,[a]}

Au nanoparticles of size 2.2 nm were encapsulated in a zeolitic imidazolate framework ZIF-8 framework (Au@ZIF-8). The composite was used as a catalyst for the selective hydrogenation of crotonaldehyde to crotyl alcohol with 90–95% selectivity. Hydrogenation of 1-hexene yielded *n*-hexane in approximately the same conversion as crotonaldehyde, whereas *cis*-cyclohexene did not detectably react. To account for the confined environment of the ZIF, we supported Au nanoparticles on the outside of ZIF-8 (Au/ZIF-8). Using Au/ZIF-8 as a catalyst, 1-hexene

and *cis*-cyclohexene were hydrogenated in low conversion whereas crotonaldehyde would only react at higher pressures in 70% selectivity towards crotyl alcohol. Post-experiment TEM analysis of Au/ZIF-8 showed significant sintering whereas the median particle size of Au@ZIF-8 remained almost unchanged. Au@ZIF-8 was recycled as a catalyst for the hydrogenation of crotonaldehyde three times without significant loss of activity or selectivity.

Introduction

As many industrially relevant precursors are derived from allylic alcohols, the chemospecific (C=O specific) hydrogenation of α,β -unsaturated ketones and aldehydes is a highly desirable chemical transformation. Traditional metals such as Ni, Pd, and Pt are potent hydrogenation catalysts, but preferentially hydrogenate the C=C bonds resulting mainly in saturated ketones and aldehydes.^[1] Notably, although both are exoergic, hydrogenation of a C=O bond is thermodynamically disfavored by 35 kJ mol⁻¹ versus that of a C=C bond. Nevertheless, nanoparticulate Au catalysts have been shown to be selective for the hydrogenation of the C=O bonds of α,β -unsaturated ketones and aldehydes.^[2]

The selectivity of Au nanoparticles as catalysts for organic reactions is influenced by many factors, including reaction conditions,^[2a] nanoparticle size and morphology,^[2a,b,3] and the type of support.^[2a,4] Nanoparticle size is thought to have perhaps the greatest influence on selectivity, with the best selectivity towards α,β -unsaturated alcohols obtained from the smallest

Au particle sizes.^[5] Although traditional Au nanoparticle catalysts have never achieved 100% selectivity towards C=O hydrogenation,^[6] selectivity towards allylic alcohols can be improved by selective chemical poisoning of specific crystallographic facets^[7] or by encapsulating the nanoparticles within the pores of zeolites.^[7b,8] Herein, we report that encapsulation of Au nanoparticle catalysts by the zeolitic imidazolate framework compound^[9] ZIF-8 greatly boosts their regio/chemoselectivity toward hydrogenation of a representative α,β -unsaturated aldehyde, crotonaldehyde, even relative to the above mentioned approaches. Indeed, the overall selectivity for allylic alcohol formation is approximately 95% and the preference for the allylic alcohol over the alkyl aldehyde product is, within experimental uncertainty, quantitative.

ZIFs belong to a class of materials known as metal-organic frameworks (MOFs).^[10,11] These versatile materials have been investigated for many potential applications including chemical separations,^[12] sensing,^[13] and catalysis.^[10b] The overall stoichiometry of homoleptic ZIFs is generally $M(\text{Im})_2$ where the node, M, is a tetrahedrally coordinated metal in oxidation state II, and the bond angle is similar to the Si–O–Si bond angle found in zeolites and, by definition, the topology of a ZIF is one known for inorganic zeolites.

The encapsulation of nanoparticles within MOFs—typically for catalysis, but also for applications such as chemical sensing^[14]—has been the subject of considerable study.^[15] The two general approaches to obtaining nanoparticle@MOF composites are: a) to form the particles within the preexisting MOF—typically by reducing metal complexes that have infiltrated the MOF pores (e.g., by chemical vapor deposition or incipient wetness impregnation),^[7b,15a,16] or b) to grow the MOF around the preexisting nanoparticle(s). The second strategy has proven increasingly popular because it allows for independent

[a] C. J. Stephenson, Prof. P. C. Stair, Prof. O. K. Farha, Prof. J. T. Hupp
Department of Chemistry
Northwestern University
2145 Sheridan Road, Evanston, IL 60208 (USA)
E-mail: j-hupp@northwestern.edu
o-farha@northwestern.edu

[b] C. L. Whitford
Department of Chemical and Biological Engineering
Northwestern University
2145 Sheridan Road, Evanston, IL 60208 (USA)

[c] Prof. O. K. Farha
Department of Chemistry
King Abdulaziz University
Jeddah (Saudi Arabia)

Supporting Information for this article is available on the WWW under <http://dx.doi.org/10.1002/cctc.201501171>.

control (precontrol) over particle size and because it typically yields pinhole-free MOF coatings—thereby ensuring that gas- or solution-phase molecules must traverse the MOF to reach a potentially catalytic or chemoresponsive particle.^[16f,i,17] Indeed, since its description for ZIF-8 and various metal, metal-oxide, and metal-sulfide nanoparticles,^[18] the approach has been extended to a variety of MOFs, including UiO-66^[17d,19] and UiO-67,^[17d] MIL-53,^[19] MOF-801,^[17d] and others.^[16f,i,17a,d,f,19,20]

ZIF-8 presents small, but flexible,^[21] apertures of crystallographic width 3.4 Å that open into cavities of diameter 11.6 Å. Recognizing that small linear alkanes, alkenes, and alcohols have kinetic diameters in the range of approximately 4.4–6 Å, crotonaldehyde is expected to pass through the apertures. In turn, at the ZIF-8/gold-nanoparticle interface, only the permeating molecule's terminus would be able to contact the enshrouded particle's surface. This could provide a basis for chemoselective (aldehyde selective) hydrogenation of crotonaldehyde to yield crotyl alcohol. We previously observed that ZIF-8-encapsulated platinum nanoparticles display superb regioselectivity towards terminal olefins in the hydrogenation of linear alkenes and alkynes.^[18,22] Although Pt@ZIF-8 composites should be capable of regioselectively catalyzing the hydrogenation of crotonaldehyde, decarbonylation forms CO, which readily adsorbs and poisons Pt surfaces. Gold nanoparticles, in contrast, resist CO poisoning,^[23,24] making them attractive as catalytic encapsulants.

Results and Discussion

Poly(vinylpyrrolidone) (PVP) coated Au nanoparticles were synthesized by using a procedure adapted from the literature (see Experimental Section).^[25] From transmission electron microscopy (TEM) (see Supporting Information Figure S1) measurements, the particles averaged 1.6 nm in diameter, with the vast majority below 2 nm (and a smaller number of ≈ 4 nm). The Au@ZIF-8 composite was synthesized by the addition of methanolic solutions of zinc nitrate and linker followed by addition of a dilute ($0.22 \text{ mg}_{\text{Au}} \text{ mL}^{-1}$) aqueous solution of Au nanoparticles. The brown Au@ZIF-8 composite was characterized by scanning transmission electron microscopy (STEM), inductively coupled plasma atomic emission spectroscopy (ICP-AES), and powder X-ray diffraction (PXRD) measurements. The Au content was found to be approximately 0.6 wt.% by ICP-AES. STEM revealed crystallites of approximately 400–600 nm size (Figure 1a and Figure S3). From STEM of Au@ZIF-8, the Au nanoparticles were of average particle diameter of 2.5 nm with a median particle diameter of 2.2 nm (Figure 1a and 1b). The smallest observed particle was approximately 1.1 nm and the largest was approximately 6 nm.

As a control for ZIF environmental effects other than confinement, we also immobilized Au nanoparticles on the exterior surface of the MOF (Au/ZIF-8). Electron microscopy revealed a composite consisting of ZIF-8 crystallites of approximately 200 nm, with Au nanoparticles of 2–5 nm diameter (plus a few nanoparticles greater than 5 nm) sited on the crystallite surface (Figure 1c and 1d). Although one might anticipate interference by PVP, for example, substrate binding, it has been shown else-

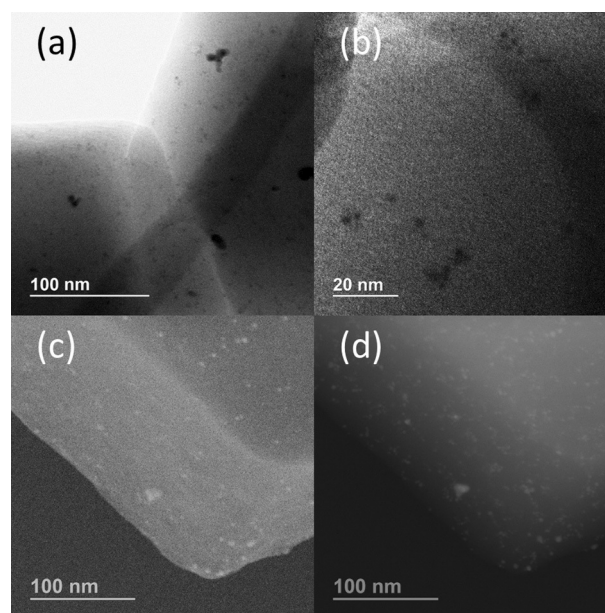


Figure 1. TEM images of a) Au@ZIF-8 showing Au nanoparticles encapsulated in ZIF crystallites and b) higher magnification image of Au@ZIF-8 showing small Au nanoparticles in a single ZIF crystallite; STEM images of Au/ZIF-8 showing Au nanoparticles on the exterior of ZIF-8 crystallite in c) scanning mode and d) Z-contrast mode.

where that PVP-coated Au nanoparticles are active for the hydrogenation of α,β -unsaturated aldehydes.^[3c]

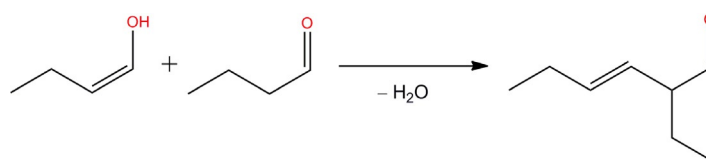
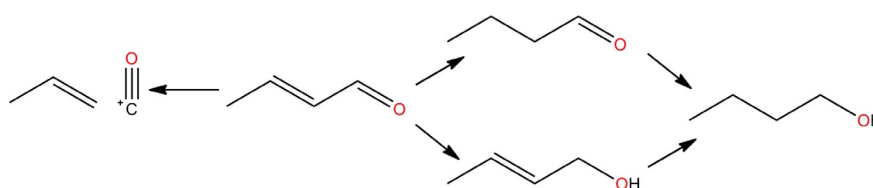
Catalytic hydrogenation runs were conducted in a 25 mL Parr bomb with 3.6 mL solvent (THF or ethanol) with 2000 equivalents of substrate, under 5 bar of H₂ for 24 h at 80 °C, using 0.200 mL undecane as an internal standard (Table 1). To gauge whether nanoparticles were fully encapsulated and that pinhole defects in the MOF were absent, we first evaluated the substrate-size selectivity of the composite catalyst. As anticipated for well-encapsulated active sites, *cis*-cyclohexene proved unreactive if exposed under H₂ to Au@ZIF-8. In contrast, under the same conditions exposure to Au/ZIF-8 converted *cis*-cyclohexene to cyclohexane with 4% initial yield (Table 1, entries 1 and 2), demonstrating that exposed nanoparticles are indeed catalytically competent for alkene hydrogenation. Thus, the absence of reactivity in the presence of Au@ZIF-8 can be ascribed to substrate exclusion. Extending the comparison to 1-hexene, a candidate reactant that is known to be capable of permeating ZIF-8, we observed 30% conversion to *n*-hexane with Au/ZIF-8 as the catalyst, but only 10% conversion with Au@ZIF-8 (entries 2 and 3). The difference can be viewed as an indication of the extent to which the rate of reactant transport through the MOF limits the kinetics of composite-catalyzed hydrogenation. To access the composite material's ability to hydrogenate internal C=C unsaturated bonds, we performed hydrogenations with Au@ZIF-8 and Au/ZIF-8 with *trans*-3-hexene as a substrate. The substrate went unreacted with Au@ZIF-8 as a catalyst (entry 5) whereas Au/ZIF-8 hydrogenated *trans*-3-hexene to *n*-hexane in 10% conversion (entry 6).

Table 1. Catalytic results for the hydrogenation of unsaturated substrates using Au@ZIF-8, Au/ZIF-8, Au₆@ZIF-8, or Au₆/ZIF-8 as catalysts.^[a]

Entry	Catalyst	Substrate	Product	Conversion ^[b,c] [%]	Selectivity ^[b,c] [%]
1	Au@ZIF-8			0	–
2	Au/ZIF-8			4	–
3	Au@ZIF-8			10	–
4	Au/ZIF-8			30	–
5	Au@ZIF-8			0	–
6	Au/ZIF-8			10	–
7	Au@ZIF-8			13	93
8	Au/ZIF-8			–	–
9 ^[d]	Au/ZIF-8			50	70
10 ^[d]	Au ₆ @ZIF-8			20	85
11 ^[d]	Au ₆ /ZIF-8			80	50
12 ^[e]	Au@ZIF-8			11	90
13 ^[e]	Au@ZIF-8			14	95
14 ^[e]	Au@ZIF-8			9	89

[a] General catalytic conditions: 2000 equivalents of substrate in 3.6 mL solvent with 0.200 mL undecane as an internal standard at 80 °C under 5 bar H₂ performed in duplicate. [b] Determined by GC-TOF or GC-FID techniques. [c] Selectivity relative to all reported products. [d] Performed under 15 bar H₂. [e] Performed by reusing the same catalyst sample.

For crotonaldehyde, Au@ZIF-8 catalyzed its hydrogenation with 93% selectivity for the desired allylic alcohol (Table 1, entry 7). Zero amounts of butyraldehyde were detected, suggesting quantitative selectivity for C=O hydrogenation relative to C=C hydrogenation. Also detected, however, were small amounts of side products having masses matching those of dimers of butyraldehyde. Butyraldehyde can form from C=C hydrogenation of crotonaldehyde or from keto–enol tautomerization of crotyl alcohol (Scheme 2). The side products presumably arise from aldol condensation of butyraldehyde. We conclude, therefore, that the observed overall selectivity of 95% for hydrogenation of the aldehyde portion of crotonaldehyde is likely also the initial selectivity for C=O versus C=C hydrogenation. Consistent with this notion, no evidence was found for formation of a third primary product (such as propene; Scheme 1). Finally, notably the surface sites of ZIF-8 (presumably including non-coordinated nitrogen atoms of 2-methyl-imidazolates) are known to be catalytically active for aldol condensations.^[26]

**Scheme 2.** Aldol condensation reaction between crotyl alcohol and butyrylaldehyde.**Scheme 1.** Possible hydrogenation products and decarbonylation pathway for crotonaldehyde.

From the literature, the selectivity of non-encapsulated gold nanoparticles for the unsaturated alcohol product in the catalysis of hydrogenation of α,β -unsaturated alcohols is strongly dependent on nanoparticle size. Bus et al. examined alumina-supported Au nanoparticles of various sizes for the liquid phase hydrogenation of cinnamaldehyde (80 bar H₂; 100 °C). For 1–2 nm nanoparticles, they reported 90% selectivity for the allylic alcohol, with selectivity decreasing sharply with increasing particle size.^[27] Zanella et al. looked at titania-supported Au nanoparticles (1–2 nm) on titania for the gas-phase hydrogenation of crotonaldehyde at 120 °C.^[28] The highest selectivity observed for crotyl alcohol was approximately 70%.^[28] Volpe explored the hydrogenation of crotonaldehyde over Au/CeO₂ catalysts in the gas phase and found that high selectivity (73%) was obtained with the smallest particles (sub 4 nm).^[4b,29] Intriguingly, if the Au/CeO₂ catalysts were used in the liquid phase, the highest selectivity obtained was 29%.^[29b] The drop in selectivity was attributed to competitive adsorption of solvent and other products. This highlights the importance of encapsulation as a means of protecting the nanoparticle surface from reactants that might be detrimental to selectivity. Given the distribution of particle sizes in our composites, it is conceivable that the approximately 5% diversion away from crotyl alcohol and toward butyraldehyde-

derived products, is the result of comparatively unselective hydrogenation catalysis by larger particles. If so, then even higher selectivities for crotyl alcohol (i.e., > 95%) would be obtained if composites containing only the smallest catalytic particles could be used. Regardless, the selectivity that we observe for the allylic alcohol is among the highest reported for the hydrogenation of crotonaldehyde.^[5,6,30]

We prepared a ZIF-8 composite with approximately 6–10 nm Au nanoparticles encapsulated within to investigate the effect of particle size on selectivity in crotonaldehyde hydrogenation (Au₆@ZIF-8, Figure 2a and Figure 2b). We also prepared a control catalyst with 6–10 nm Au nanoparticles on the exterior of

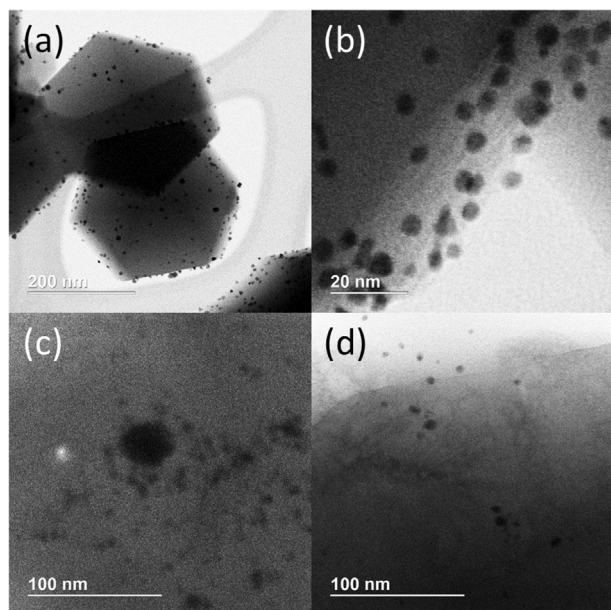


Figure 2. TEM images of a) multiple Au₆/ZIF-8 crystallites showing Au nanoparticles 6–10 nm on the exterior of ZIF crystallites; b) Au₆/ZIF-8 showing Au nanoparticles; c) Au₆@ZIF-8 showing 6–10 nm Au nanoparticles encapsulated in ZIF-8 crystallite; d) Au₆@ZIF-8 showing Au nanoparticles in ZIF-8 crystallite.

the ZIF-8 framework (Au₆/ZIF-8 Figure 2c and 2d). The hydrogenation of crotonaldehyde was carried out at elevated pressure (15 bar H₂). For Au₆/ZIF-8, selectivity towards crotyl alcohol is approximately 50% with a large amount of aldol condensation products and *n*-butanol as the main side-products (Table 1, entry 11). Au₆@ZIF-8 converted 20% of crotonaldehyde to crotyl alcohol with 85% selectivity (entry 12). This result indicates that the selectivity that we obtain with Au@ZIF-8 might be attributed to the confined environment of the ZIF and not strictly to particle size alone. Similarly, Rojas et al. supported 6 nm Au nanoparticles on silica for the liquid-phase hydrogenation of cinnamaldehyde at 80 °C and obtained a selectivity of 80%.^[31]

For the attempted hydrogenation of crotonaldehyde using Au/ZIF-8 as a catalyst, we observed no conversion (Table 1, entry 8). The failure was accompanied by a change in catalyst color from brown to pink (Figure S5; in contrast, the color of Au@ZIF-8 was unchanged). The pink color is suggestive of particle aggregation and indeed TEM indicated a substantial increase in particle size (to 6 nm, Figure 3b) with some exceeding 15 nm. In contrast, for Au@ZIF-8 we saw no change in median particle diameter (2.2 nm, Figure 3a) and only a small increase in average particle size (2.5 nm to 3.3 nm). This difference might or might not be statistically meaningful and, therefore, indicative of slight sintering. We then attempted the hydrogenation of crotonaldehyde at higher pressure (15 bar H₂). Under these conditions, with Au@ZIF-8 as the catalyst, we observed 30% conversion of crotonaldehyde with approximately 70% selectivity towards the allylic alcohol (Table 1, entry 9). Butyraldehyde, butanol, and aldol condensation products were the primary side products observed.

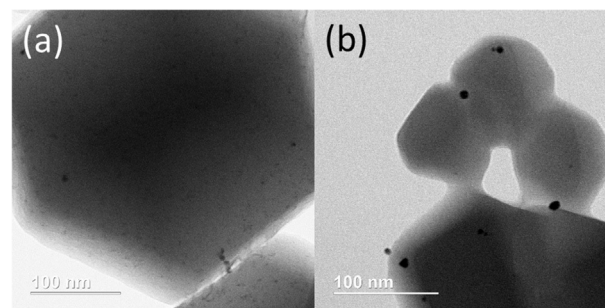


Figure 3. TEM images of a) Au@ZIF-8 post-catalysis; b) Au/ZIF-8 post-catalysis.

Given the negligible or nearly negligible changes in Au@ZIF-8 nanoparticle size during catalysis, we examined the potential of the composite for recovery and reuse. As shown in Table 1, entries 12–14, the activity and selectivity of the catalyst changed very little, if at all, over the course of four catalytic runs. (Between trials, the sample was dried overnight at 100 °C under vacuum.) In contrast, conventionally supported Au nanoparticle catalysts suffer from high rates of particle sintering and aggregation.^[23,32]

Finally, while our study was in progress we learned of similar work by Huang and coworkers.^[7b] Briefly, they examined the hydrogenation of cinnamaldehyde as catalyzed by Pt@UiO-66-NH₂. Cinnamaldehyde presents a larger steric cross-section than crotonaldehyde, but UiO-66 presents larger apertures than ZIF-8. The net result is similarly high MOF-engendered selectivity of the nanoparticle catalyst for hydrogenation of the C=O bond relative to the allyl C=C bond. However, notably the authors used 1 mL of trimethylamine in their catalytic trials, presumably to selectively poison more reactive facets and increase selectivity towards C=O hydrogenation. In our work, we only rely on the nanoparticles and the confining environment of the framework to provide selectivity.

Conclusions

Encapsulation of small Au particles (≈ 2 nm) in zeolitic imidazolate framework compound ZIF-8 renders them highly selective for aldehyde hydrogenation over internal unsaturated bond hydrogenation. Encapsulation also prevents particle agglomeration and concomitant loss of catalytic activity, enabling the catalyst to be isolated, re-suspended and reused. The observed enhanced selectivity for the formation of crotyl alcohol from crotonaldehyde is attributed to a tendency for the small-diameter apertures to permit only the termini of the reactant to reach the Au nanoparticle surface. The terminal methyl group is unreactive and the aperture-confined allyl group at the center of crotonaldehyde is unable to access the catalyst surface, leaving only the C=O group available and able to react with nanoparticle-activated hydrogen.

Experimental Section

Materials

Hydrogen tetrachloroaurate trihydrate (49% Au, 99.9% purity based on Au) and zinc nitrate hexahydrate (98%) was purchased from Strem Chemicals; Au ICP standard, poly(vinylpyrrolidone) powder, (K30, MW 40 000; MW 10 000), 2-methylimidazole (99%), 1-hexene (99.9%), *trans*-3-hexene (99.9%), *cis*-cyclohexene (>99%), crotonaldehyde (98% predominantly *trans*), undecane ($\geq 99\%$), ethanol (anhydrous, $\geq 99.5\%$), diethyl ether (ACS reagent, $\geq 99\%$), nitric acid (traceSELECT for trace analysis), hydrochloric acid (ACS reagent grade, 37%), tetrahydrofuran (>99.9%, anhydrous), and methanol (HPLC grade, 99.99%) were purchased from Sigma Aldrich; Microsep Advanced Filter Devices (30k cutoff) were purchased from Pall Life Sciences; hydrogen for catalytic experiments (UHP, 99.999%) was purchased from Airgas; TEM grids (300 mesh Cu/lacey carbon; 400 mesh, Cu/C) were purchased from Ted Pella.

Physical and analytical measurements

Gas chromatography time-of-flight (GC-TOF) data were recorded on a Waters Micromass GCT Premiere with an Agilent 7890 GC inlet and a DB5 30 meter column in EI mode. Samples were diluted in 1 mL diethyl ether. GC-FID data were recorded on an Agilent 7820A with a 19091 J-413 column. TEM was performed on a Hitachi H-8100 Microscope. STEM was performed on a Hitachi HD-2300 Dual EDS Cryo STEM at 200 kV. Samples for STEM analysis were prepared by dropping a methanolic solution of the compound onto Cu/C TEM grids or lacey carbon TEM grids. ICP-AES was performed on a Varian Vista MPX ICP spectrometer. Samples were digested in aqua regia and diluted in Milli-Q water. PXRD analysis was performed on a Rigaku Smartlab Thin-film Diffraction WorkStation with 9 kW copper rotation anode X-ray source coupled with a multilayer optic. Spectra were recorded from $2^\circ < \theta < 70^\circ$.

Synthesis of sub 2 nm Au-PVP nanoparticles

The Au nanoparticles were synthesized by a procedure adapted from the literature.^[25] HAuCl₄·3H₂O (20.0 mg, 0.051 mmol) and PVP (MW 40 000; 555 mg) in 50 mL water were stirred in an ice-water bath for 20 min before NaBH₄ (20 mg, 0.95 mmol) in 5 mL H₂O was rapidly added to the stirring solution. The solution changed color from yellow to brown indicating the formation of small Au nanoparticles. After stirring for 20 min, chilled acetone was added to precipitate nanoparticles. The nanoparticles were isolated by centrifugation and then dissolved in ice-cold water and subjected to filtration using a Pall Life Sciences Microsep Advanced Filter Devices (30k cutoff). The solution/suspension was kept in an ice-water bath throughout the purification process.

Synthesis of 6 nm Au-PVP nanoparticles

Larger Au nanoparticles were synthesized by adapted literature methods.^[33] HAuCl₄·3H₂O (10.0 mg, 0.025 mmol) was dissolved in 5 mL Millipore water. PVP (MW 10 000; 62 mg) was dissolved in 90 mL ethylene glycol and heated at 80 °C for 2 h. The solution of gold chloride was added to the PVP solution at 0 °C. The pH was adjusted to 9 by the addition of 1 M NaOH (1 M in Millipore water). The reaction was then stirred at 100 °C for 90 min. The pink solution was cooled to RT and subsequently subjected to filtration using a Pall Life Sciences Microsep Advanced Filter Deice (30k cutoff) and then diluted to 0.2 mg mL⁻¹ Au in with water.

Synthesis of Au@ZIF-8 composites

Au@ZIF-8 composites were prepared by modifying the literature procedure. Methanolic solutions of zinc nitrate hexahydrate (500 mL, 15 mM) and 2-methylimidazole (500 mL, 15 mM) were mixed in a 250 mL Erlenmeyer flask, followed by the immediate addition of PVP-coated Au nanoparticles. The solution slowly became opaque and a light brown precipitate slowly formed. After standing for approximately 24 h, the precipitate was isolated by centrifugation and washed several times with methanol. In between washings, the solid was allowed to soak in solvent for a few hours. The solid was dried under vacuum, overnight.

Synthesis of Au/ZIF-8

ZIF-8 (200 mg) was stirred with Au-PVP (2 mg Au) in 20 mL H₂O in 50 mL DMF for 2 h. The brown solid was isolated by centrifugation, washed twice with DMF and then ethanol, and dried under vacuum at 80 °C overnight.

Catalytic trials

Catalytic hydrogenations were conducted in a 25 mL Parr bomb with 3.6 mL solvent (THF or ethanol) with 2000 equivalents of substrate, under 5 bar of H₂. Au@ZIF-8 or Au/ZIF-8 were first heated at 120 °C under vacuum for 2 h. Samples were then reduced under a H₂ atmosphere for 2 h at 120 °C. The catalyst and reaction solvent were loaded into the reactor under an inert atmosphere. The Parr reactor was then interfaced to a Schlenk line and cooled in a dry ice/acetone bath. The reaction solution was subjected to two or three freeze-pump-thaw cycles. The reactor was then placed in an 80 °C oil bath. The system was equilibrated before introducing H₂. Samples were analyzed by taking an aliquot, diluting it in 1 mL diethyl ether before analyzing it by GC.

Acknowledgements

We gratefully acknowledge financial support from the National Science Foundation (DMR-1334928). Acquisition of data on trace analysis, GC instruments, and X-ray used in the IMSERC facility of Northwestern University was made possible by support from Northwestern University and grant CHE-0923236 from the National Science Foundation, respectively. This work made use of the TEM and STEM instruments located in the EPIC facility (NUANCE Center-Northwestern University), which has received support from the MRSEC program (NSF DMR-1121262) at the Materials Research Center; the Nanoscale Science and Engineering Center (NSF EEC-0647560) at the International Institute for Nanotechnology; and the State of Illinois, through the International Institute for Nanotechnology.

Keywords: aldehydes · chemoselectivity · gold · hydrogenation · metal-organic frameworks

[1] H. Pines in *The Chemistry of Catalytic Hydrocarbon Conversions* (Ed.: H. Pines), Academic Press, New York, **1981**.

[2] a) S. Schimpf, M. Lucas, C. Mohr, U. Rodemerck, A. Brückner, J. Radnik, H. Hofmeister, P. Claus, *Catal. Today* **2002**, *72*, 63–78; b) M. C. Daniel, D. Astruc, *Chem. Rev.* **2004**, *104*, 293–346; c) P. Claus, *Appl. Catal. A* **2005**, *291*, 222–229; d) A. S. K. Hashmi, *Chem. Rev.* **2007**, *107*, 3180–3211; e) Y.

- Zhang, X. Cui, F. Shi, Y. Deng, *Chem. Rev.* **2012**, *112*, 2467–2505; f) M. Juliusa, S. Roberts, J. Q. Fletcher, *Gold Bull.* **2010**, *43*, 298–306.
- [3] a) P. Claus, A. Brückner, C. Mohr, H. Hofmeister, *J. Am. Chem. Soc.* **2000**, *122*, 11430–11439; b) A. Corma, M. Boronat, S. Gonzalez, F. Illas, *Chem. Commun.* **2007**, 3371–3373; c) P. G. N. Mertens, P. Vandezande, X. Ye, H. Poelman, I. F. J. Vankelecom, D. E. De Vos, *Appl. Catal. A* **2009**, *355*, 176–183; d) A. Noujima, T. Mitsudome, T. Mizugaki, K. Jitsukawa, K. Kaneda, *Chem. Commun.* **2012**, *48*, 6723–6725.
- [4] a) C. Milone, R. Ingoglia, L. Schippilli, C. Crisafulli, G. Neri, S. Galvagno, *J. Catal.* **2005**, *236*, 80–90; b) B. Campo, G. Santori, C. Petit, M. Volpe, *Appl. Catal. A* **2009**, *359*, 79–83; c) K. J. You, C. T. Chang, B. J. Liaw, C. T. Huang, Y. Z. Chen, *Appl. Catal. A* **2009**, *361*, 65–71; d) L. Delannoy, G. Thrimurthulu, P. S. Reddy, C. Methivier, J. Nelayah, B. M. Reddy, C. Ricolleau, C. Louis, *Phys. Chem. Chem. Phys.* **2014**, *16*, 26514–26527.
- [5] T. Mitsudome, K. Kaneda, *Green Chem.* **2013**, *15*, 2636–2654.
- [6] Y. Zhu, H. Qian, B. A. Drake, R. Jin, *Angew. Chem. Int. Ed.* **2010**, *49*, 1295–1298; *Angew. Chem.* **2010**, *122*, 1317–1320.
- [7] a) J. E. Bailie, G. J. Hutchings, *Chem. Commun.* **1999**, 2151–2152; b) Z. Guo, C. Xiao, R. V. Maligal-Ganesh, L. Zhou, T. W. Goh, X. Li, D. Tesfagaber, A. Thiel, W. Huang, *ACS Catal.* **2014**, *4*, 1340–1348.
- [8] D. G. Blackmond, R. Oukaci, B. Blanc, P. Gallezot, *J. Catal.* **1991**, *131*, 401–411.
- [9] a) A. Phan, C. J. Doonan, F. J. Uribe-Romo, C. B. Knobler, M. O’Keeffe, O. M. Yaghi, *Acc. Chem. Res.* **2010**, *43*, 58–67; b) J. P. Zhang, Y. B. Zhang, J.-B. Lin, X.-M. Chen, *Chem. Rev.* **2012**, *112*, 1001–1033; c) H. Hayashi, A. P. Cote, H. Furukawa, M. O’Keeffe, O. M. Yaghi, *Nat. Mater.* **2007**, *6*, 501–506; d) K. S. Park, Z. Ni, A. P. Côté, J. Y. Choi, R. Huang, F. J. Uribe-Romo, H. K. Chae, M. O’Keeffe, O. M. Yaghi, *Proc. Natl. Acad. Sci. USA* **2006**, *103*, 10186–10191; e) B. Chen, Z. Yang, Y. Zhu, Y. Xia, *J. Mater. Chem. A* **2014**, *2*, 16811–16831.
- [10] a) O. K. Farha, J. T. Hupp, *Acc. Chem. Res.* **2010**, *43*, 1166–1175; b) D. Farusseng, S. Aguado, C. Pinel, *Angew. Chem. Int. Ed.* **2009**, *48*, 7502–7513; *Angew. Chem.* **2009**, *121*, 7638–7649; c) H.-C. Zhou, J. R. Long, O. M. Yaghi, *Chem. Rev.* **2012**, *112*, 673–674; d) J. Lee, O. K. Farha, J. Roberts, K. A. Scheidt, S. T. Nguyen, J. T. Hupp, *Chem. Soc. Rev.* **2009**, *38*, 1450–1459; e) J. R. Long, O. M. Yaghi, *Chem. Soc. Rev.* **2009**, *38*, 1213–1214; f) L. Ma, C. Abney, W. Lin, *Chem. Soc. Rev.* **2009**, *38*, 1248–1256; g) H. Furukawa, K. E. Cordova, M. O’Keeffe, O. M. Yaghi, *Science* **2013**, *341*, 1230444.
- [11] X. C. Huang, Y. Y. Lin, J. P. Zhang, X.-M. Chen, *Angew. Chem. Int. Ed.* **2006**, *45*, 1557–1559; *Angew. Chem.* **2006**, *118*, 1587–1589.
- [12] D. Peralta, G. Chaplais, A. Simon-Masseron, K. Barthelet, C. Chizallet, A.-A. Quoineaud, G. D. Pirngruber, *J. Am. Chem. Soc.* **2012**, *134*, 8115–8126.
- [13] G. Lu, J. T. Hupp, *J. Am. Chem. Soc.* **2010**, *132*, 7832–7833.
- [14] a) S. Li, F. Huo, *Nanoscale* **2015**, *7*, 7482–7501; b) Y. Zhao, N. Kornienko, Z. Liu, C. Zhu, S. Asahina, T.-R. Kuo, W. Bao, C. Xie, A. Hexemer, O. Terasaki, P. Yang, O. M. Yaghi, *J. Am. Chem. Soc.* **2015**, *137*, 2199–2202; c) P. Falcaro, R. Ricco, A. Yazdi, I. Imaz, S. Furukawa, D. Maspoch, R. Ameloot, J. D. Evans, C. J. Doonan, *Coord. Chem. Rev.* **2015**, *307*, 237–254.
- [15] a) H. R. Moon, D.-W. Lim, M. P. Suh, *Chem. Soc. Rev.* **2013**, *42*, 1807–1824; b) A. Aijaz, Q. Xu, *J. Phys. Chem. Lett.* **2014**, *5*, 1400–1411; c) Q.-L. Zhu, Q. Xu, *Chem. Soc. Rev.* **2014**, *43*, 5468–5512; d) C. Rösler, R. A. Fischer, *CrystEngComm* **2015**, *17*, 199–217.
- [16] a) D. Esken, S. Turner, C. Wiktor, S. B. Kalidindi, G. Van Tenderloo, R. A. Fischer, *J. Am. Chem. Soc.* **2011**, *133*, 16370; b) H. L. Jiang, B. Liu, T. Akita, M. Haruta, H. Sakurai, Q. Xu, *J. Am. Chem. Soc.* **2009**, *131*, 11302–11303; c) D. Esken, S. Turner, O. I. Lebedev, G. Van Tendeloo, R. A. Fischer, *Chem. Mater.* **2010**, *22*, 6393–6401; d) Y. Huang, Z. Lin, R. Cao, *Chem. Eur. J.* **2011**, *17*, 12706–12712; e) J. Hermannsdörfer, M. Friedrich, N. Miyajima, R. Q. Albuquerque, S. Kümmel, R. Kempe, *Angew. Chem. Int. Ed.* **2012**, *51*, 11473–11477; *Angew. Chem.* **2012**, *124*, 11640–11644; f) C. Hou, G. Zhao, Y. Ji, Z. Niu, D. Wang, Y. Li, *Nano Res.* **2014**, *7*, 1364–1369; g) X. Li, Z. Guo, C. Xiao, T. W. Goh, D. Tesfagaber, W. Huang, *ACS Catal.* **2014**, *4*, 3490–3497; h) Y. Luan, Y. Qi, H. Gao, N. Zheng, G. Wang, *J. Mater. Chem. A* **2014**, *2*, 20588–20596; i) C. Rösler, D. Esken, C. Wiktor, H. Kobayashi, T. Yamamoto, S. Matsumura, H. Kitagawa, R. A. Fischer, *Eur. J. Inorg. Chem.* **2014**, 5514–5521; j) K. Leus, P. Concepcion, M. Vandichel, M. Meledina, A. Grrirrane, D. Esquivel, S. Turner, D. Poelman, M. Waroquier, V. Van Speybroeck, G. Van Tendeloo, H. Garcia, P. Van Der Voort, *RSC Adv.* **2015**, *5*, 22334–22342.
- [17] a) P. Wang, J. Zhao, X. Li, Y. Yang, Q. Yang, C. Li, *Chem. Commun.* **2013**, 49, 3330–3332; b) P. Hu, J. Zhuang, L. Y. Chou, H. K. Lee, X. Y. Ling, Y. C. Chuang, C.-K. Tsung, *J. Am. Chem. Soc.* **2014**, *136*, 10561–10564; c) K. Na, K. M. Choi, O. M. Yaghi, G. A. Somorjai, *Nano Lett.* **2014**, *14*, 5979–5983; d) M. Sadakiyo, M. Kon-no, K. Sato, K. Nagaoka, H. Kasai, K. Kato, M. Yamauchi, *Dalton Trans.* **2014**, 43, 11295–11298; e) M. Zhang, Y. Yang, C. Li, Q. Liu, C. T. Williams, C. Liang, *Catal. Sci. Technol.* **2014**, *4*, 329–332.
- [18] G. Lu, S. Li, Z. Guo, O. K. Farha, B. G. Hauser, X. Qi, Y. Wang, X. Wang, S. Han, X. Liu, J. S. DuChene, H. Zhang, Q. Zhang, X. Chen, J. Ma, S. C. J. Loo, W. D. Wei, Y. Yang, J. T. Hupp, F. Huo, *Nat. Chem.* **2012**, *4*, 310–316.
- [19] W. Zhang, G. Lu, C. Cui, Y. Liu, S. Li, W. Yan, C. Xing, Y. R. Chi, Y. Yang, F. Huo, *Adv. Mater.* **2014**, *26*, 4056–4060.
- [20] K. Khaletskaya, A. Pougin, R. Medishetty, C. Rösler, C. Wiktor, J. Strunk, R. A. Fischer, *Chem. Mater.* **2015**, *27*, 7248–7257.
- [21] a) D. Fairen-Jimenez, S. A. Moggach, M. T. Wharmby, P. A. Wright, S. Parsons, T. Düren, *J. Am. Chem. Soc.* **2011**, *133*, 8900–8902; b) K. Zhang, R. P. Lively, C. Zhang, R. R. Chance, W. J. Koros, D. S. Sholl, S. Nair, *J. Phys. Chem. Lett.* **2013**, *4*, 3618–3622.
- [22] C. J. Stephenson, J. T. Hupp, O. K. Farha, *Inorg. Chem. Front.* **2015**, *2*, 448–452.
- [23] C. H. Bartholomew, *Appl. Catal. A* **2001**, *212*, 17–60.
- [24] M. Boronat, P. Concepción, A. Corma, *J. Phys. Chem. C* **2009**, *113*, 16772–16784.
- [25] H. Tsunoyama, H. Sakurai, N. Ichikuni, Y. Negishi, T. Tsukuda, *Langmuir* **2004**, *20*, 11293–11296.
- [26] a) C. Chizallet, S. Lazare, D. Bazer-Bachi, F. Bonnier, V. Lecocq, E. Soyer, A.-A. Quoineaud, N. Bats, *J. Am. Chem. Soc.* **2010**, *132*, 12365–12377; b) A. Dhakshinamoorthy, M. Opanasenko, J. Čejka, H. Garcia, *Adv. Synth. Catal.* **2013**, *355*, 247–268; c) H. Fan, Y. Yang, J. Song, G. Ding, C. Wu, G. Yang, B. Han, *Green Chem.* **2014**, *16*, 600–604.
- [27] E. Bus, R. Prins, J. A. van Bokhoven, *Catal. Commun.* **2007**, *8*, 1397–1402.
- [28] R. Zanella, C. Louis, S. Giorgio, R. Touroude, *J. Catal.* **2004**, *223*, 328–339.
- [29] a) B. Campo, M. Volpe, S. Ivanova, R. Touroude, *J. Catal.* **2006**, *242*, 162–171; b) B. Campo, C. Petit, M. A. Volpe, *J. Catal.* **2008**, *254*, 71–78.
- [30] X. Liu, L. He, Y.-M. Liu, Y. Cao, *Acc. Chem. Res.* **2014**, *47*, 793–804.
- [31] H. Rojas, G. Díaz, J. J. Martínez, C. Castañeda, A. Gómez-Cortés, J. Arenas-Alatorre, *J. Mol. Catal. A* **2012**, *363*–364, 122–128.
- [32] a) J. Gong, *Chem. Rev.* **2012**, *112*, 2987–3054; b) R. Burch, *Phys. Chem. Chem. Phys.* **2006**, *8*, 5483–5500.
- [33] P. Abdulkin, T. L. Precht, B. R. Knappett, H. E. Skelton, D. A. Jefferson, A. E. H. Wheatley, *Part. Part. Syst. Character.* **2014**, *31*, 571–579.

Received: October 27, 2015

Published online on January 20, 2016